Suppression of Microbunching Instability Using Bending Magnets in Free-Electron-Laser Linacs

Ji Qiang, Chad E. Mitchell, and Marco Venturini

Lawrence Berkeley National Laboratory, Berkeley, California 94720, USA

The microbunching instability driven by collective effects of the beam inside an accelerator can significantly degrade the final electron beam quality for free electron laser (FEL) radiation. In this Letter, we propose an inexpensive scheme to suppress such an instability in accelerators for next generation FEL light sources. Instead of using an expensive device such as a laser heater or RF deflecting cavities, this scheme uses longitudinal mixing associated with the transverse spread of the beam through bending magnets inside the accelerator transport system to suppress the instability. The final uncorrelated energy spread increases roughly by the current compression factor, which is important in seeded FEL schemes in order to achieve high harmonic short-wavelength x-ray radiation.

PACS numbers: 29.27.−a, 41.60.Cr

Next generation x-ray free electron lasers (FELs) have important applications in biology, chemistry, condensed matter physics, and material science. The performance of these FELs depends critically on the quality of the electron beam used to generate the x-ray radiation. One of the factors limiting beam quality is a microbunching instability caused by collective effects (primarily longitudinal space charge) that develops as the beam is accelerated, compressed, and transported through the FEL driver. The instability can considerably magnify small current fluctuations and energy modulations that are unavoidably present in the electron beam [1–5]. In a long drift, these modulations produce modulations of the electron energy along the length of the bunch due to the effects of longitudinal space charge. After passing through a region of nonzero R_{56}, these modulations in energy result in density modulations that amplify the density modulations initially present in the beam.

The conventional method to control the instability uses a "laser heater," which consists of a laser interacting with the electron beam along an undulator located in the middle of a small chicane [2,6]. The laser heater works by enlarging the beam uncorrelated energy spread to suppress the microbunching instability through longitudinal mixing. While effective, the use of a laser heater comes at the price of reduced beam brightness due to an enlarged uncorrelated energy spread, which can compromise the machine performance. For instance, the beam brightness limits the shortest radiation wavelength achievable by seeded FELs [7]. Recently, a "reversible heating" device based on RF deflecting cavities was proposed to suppress the microbunching instability [8] without sacrificing the beam brightness. Unfortunately, the scheme would be quite expensive, and it involves significant technical complications.

In this Letter, we propose a simple method that would similarly preserve the longitudinal beam brightness, while avoiding the complication of additional and expensive hardware. The method exploits longitudinal mixing derived, not from a large beam energy spread, but from the natural transverse spread of the beam. For an upright (Twiss parameter $\alpha_{x0} = 0$) flattop electron beam with an initial current modulation b_0, passing through a horizontal bending magnet, the current modulation factor b at the exit of the bending magnet, neglecting collective effects, will be [4,9,10]

$$b(k) = b_0(k_0) \exp\left(-\frac{k^2 R_{56}^2 \sigma_{\delta 0}^2}{2}\right)$$
$$\times \exp\left(-\frac{k^2(R_{51}^2 \sigma_{x0}^2 + R_{52}^2 \sigma_{x'0}^2)}{2}\right), \qquad (1)$$

where k_0 and k are the modulation wave number before and after the bending magnet [$k = k_0/(1 + hR_{56})$ with h being the initial energy chirp of the beam]; σ_{x0} is the initial horizontal rms beam size, $\sigma_{x'0}$ is the initial horizontal rms divergence, $\sigma_{\delta 0}$ is the initial uncorrelated rms energy spread, and R_{51}, R_{52}, and R_{56} are the linear transfer matrix elements associated with the bending magnet. The second factor in Eq. (1) describes modulation damping due to the longitudinal mixing from the energy spread, and the third factor describes modulation damping due to the longitudinal mixing from the transverse spread. In a FEL linac, the electron beam before the low-energy compression chicane has an uncorrelated energy spread of $O(10^{-5})$ while the transverse rms size (in meters) and divergence (in radians) can be made $O(10^{-3})$ at a given location. The longitudinal mixing length ($R_{51}\sigma_{x0}$ and $R_{52}\sigma_{x0'}$) through a bending magnet from the transverse spread can be much larger than the longitudinal mixing length through a chicane from the energy spread. This suggests that the damping effect from the longitudinal mixing associated with nonzero R_{51} and R_{52} and transverse spread can be used as an effective method to suppress the microbunching instability. While a chicane was proposed to suppress the microbunching instability at the end of the linac in a previous study [11], in this Letter, we will make use of the effective longitudinal mixing derived from the transverse beam spread to suppress the instability. In the following we present a proof of principle for the proposed method based on
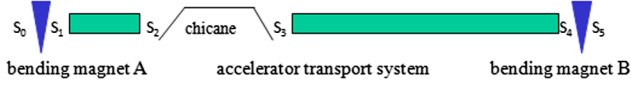
FIG. 1 (color online). A schematic plot of a general transport system between two bending magnets.

an idealized linac, a simple analytical model for the micro-bunching instability, and macroparticle simulations. Finally, we will discuss some potential challenges associated with this method.

We consider the machine layout shown in Fig. 1, consisting of a single-chicane bunch compressor with dipoles A and B placed at the two ends of the linac. Dipole A, which generates the mixing discussed above, can immediately follow the injector. An energy chirp is created in the first accelerating section to enable compression and is then removed in the second accelerator section following the chicane. Finally, dipole B has the purpose of restoring achromaticity and suppressing dispersion.

Neglecting nonlinear effects, the linear transfer matrix R through the entire system (in scaled horizontal-longitudinal coordinates that include acceleration [12]) can be written as $R = R^B T_r R^A$, where R^A and R^B are the transfer matrices for the bending magnets A and B. The transfer matrix associated with the accelerator transport system $s_1 \rightarrow s_4$ is

$$T_r = \begin{pmatrix} r_{11} & r_{12} & 0 & 0 \\ r_{21} & r_{22} & 0 & 0 \\ 0 & 0 & 1/C & r_{56} \\ 0 & 0 & 0 & C \end{pmatrix}, \quad (2)$$

where C is the compression factor of the system. By using the symplectic condition of the transfer matrices and choosing the second bending magnet so that

$$R_{51}^B = [r_{21}(R_{52}^A R_{11}^A - R_{51}^A R_{12}^A) + r_{22}(R_{52}^A R_{21}^A - R_{51}^A R_{22}^A)]/C,$$
$$R_{52}^B = [-r_{11}(R_{52}^A R_{11}^A - R_{51}^A R_{12}^A) - r_{12}(R_{52}^A R_{21}^A - R_{51}^A R_{22}^A)]/C, \quad (3)$$

the entire transport system can be made an achromat with the linear transfer matrix

$$R_{\text{tot}} = \begin{pmatrix} R_{11} & R_{12} & 0 & 0 \\ R_{21} & R_{22} & 0 & 0 \\ 0 & 0 & 1/C & R_{56}^A/C + r_{56} + R_{56}^B C \\ 0 & 0 & 0 & C \end{pmatrix}. \quad (4)$$

Although the transfer matrix (4) has the same basic form as Eq. (2), we will see that the introduction of the initial and final dipoles suppresses the amplification of the micro-bunching due to longitudinal space charge in the linac sections.

Assuming an electron beam with zero energy chirp and an initial current modulation factor b_0 at the entrance (s_0) to the first bending magnet, the final modulation factor at the exit (s_5) of the second bending magnet can be obtained by solving the microbunching integral equation provided in Ref. [4]. Neglecting collective effects inside the bending magnets and the bunch compressor chicane, the solution is given as

$$b(k_s, s_5) = b_1(k_s, s_5) + b_2(k_s, s_5) \\ + b_3(k_s, s_5) + b_4(k_s, s_5), \quad (5)$$

where $k_s = C(s)k_0$ and $C(s)$ is the compression factor $C(s) = 1/R_{55}(s)$. Here $b_1(k_s, s_5)$ describes the evolution of the modulation factor in the absence of all collective effects, and is given as

$$b_1(k_s, s_5) = b_0 \exp[-k_0^2 C^2(s_5) R_{56}^2(s_5)\sigma_{\delta_0}^2/2]; \quad (6)$$

the second term b_2 describes the amplification of the initial microbunching due to the collective effects between s_1 and s_2 inside the accelerator system and is given as

$$b_2(k_s, s_5) = ib_0 C(s_5)k_0 R_{56}(s_{1\rightarrow 5})\frac{C(s_1)I_0}{\gamma_0 I_A} \\ \times \exp\left(\frac{-k_0^2 \mathcal{D}^2(s_5)\sigma_{\delta_0}^2}{2}\right) \\ \times \exp\left(\frac{-k_0^2 \mathcal{H} \epsilon_{x,n}}{\gamma_0}\right)\int_{s_1}^{s_2} Z(k_\tau, \tau)d\tau; \quad (7)$$

the third term b_3 describes the collective effects between s_3 and s_4, and is given as

$$b_3(k_s, s_5) = ib_0 C(s_5)k_0 R_{56}(s_{3\rightarrow 5})\frac{C(s_3)I_0}{\gamma_0 I_A} \\ \times \exp\left(\frac{-k_0^2 \mathcal{D}^2(s_{3\rightarrow 5})\sigma_{\delta_0}^2}{2}\right) \\ \times \exp\left(\frac{-k_0^2 \mathcal{H} \epsilon_{x,n}}{\gamma_0}\right)\int_{s_3}^{s_4} Z(k_\tau, \tau)d\tau; \quad (8)$$

and the last term $b_4(k_s, s_5)$ describes the coupled collective effects between the region $s_1 \rightarrow s_2$ and the region $s_3 \rightarrow s_4$ and is given as

$$b_4(k_s, s_5) = -b_0 C(s_3)C(s_5)k_0^2 R_{56}(s_{1\rightarrow 3})R_{56}(s_{3\rightarrow 5})\frac{C(s_1)C(s_3)I_0^2}{(\gamma_0 I_A)^2} \exp\left(\frac{-k_0^2 \mathcal{D}^2(s_{0\rightarrow 3\rightarrow 5})\sigma_{\delta_0}^2}{2}\right)\exp\left(\frac{-k_0^2 \mathcal{H} \epsilon_{x,n}}{\gamma_0}\right) \\ \times \int_{s_1}^{s_2} Z(k_\tau, \tau)d\tau \int_{s_3}^{s_4} Z(k_\tau, \tau)d\tau. \quad (9)$$

The damping to the modulation amplification terms (b_2, b_3, b_4) is controlled by the exponents

$$\mathcal{D}^2(s_5) = U^2(s_5, s_1) + C^2(s_1)R_{56}^2(s_1),$$
$$\mathcal{D}^2(s_{3\to5}) = U^2(s_5, s_3) + C^2(s_3)R_{56}^2(s_3),$$
$$\mathcal{D}^2(s_{0\to3\to5}) = U^2(s_5, s_3) + U^2(s_3, s_1) + C^2(s_1)R_{56}^2(s_1),$$
$$\mathcal{H} = \frac{[\beta_{x0}R_{51}^A - \alpha_{x0}R_{52}^A]^2 + (R_{52}^A)^2}{\beta_{x0}}, \tag{10}$$

where $U(s, \tau) = C(s)R_{56}(s) - C(\tau)R_{56}(\tau)$, I_0 is the initial peak current, I_A is the Alfvén current, γ_0 is the initial relativistic factor, $\epsilon_{x,n}$ is the normalized horizontal emittance, $\sigma_{\delta0}$ is the initial rms relative energy spread, and $Z(k_\tau, \tau)$ is the impedance associated with collective effects such as the space-charge effect. Besides the damping effect that results from the initial energy spread and the function $\mathcal{D}$, the collective effects are also damped by the longitudinal mixing associated with the initial horizontal emittance and the function $\mathcal{H}$ [4], where β_{x0} and α_{x0} are the initial horizontal Twiss parameters. Figure 2 illustrates the final microbunching gain $|b(k_s, s_5)/b_0|$ driven by the longitudinal space-charge impedance [13] using the parameters of the following example. The result is shown as a function of the uncompressed wavelength $\lambda_0 = 2\pi/k_0$. The microbunching gain in the presence of dipoles A and B is completely suppressed relative to the gain that is obtained without the use of those magnets.

As an illustration of the above method, we assumed that an accelerator transport system consists of a 22.5 m long constant focusing channel, followed by a 10.6 m bunch compressor chicane and another 170 m constant focusing channel as shown in Fig. 1. The focusing wave numbers in the first section and the second section are about 0.63/m. The bunch compressor chicane has a momentum compaction factor of $R_{56} = 0.1$ m and provides a total compression factor of about 10. The first bending magnet has a length of 0.47 m with a bending angle of 3.9°. The second bending magnet has a length of 0.1 m with a bending angle of 0.22° according to Eq. (3). The electron beam entering the system has a total charge of 300 pC with a flattop
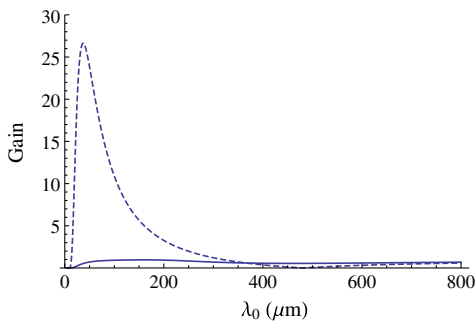
current of 50 A at 100 MeV kinetic energy. This beam is linearly accelerated in sections one and two with a linear accelerating gradient of about 10 MV/m. The final energy of the beam is about 2.1 GeV. The initial relative energy deviation chirp of the beam is zero, and it is linearly ramped up to about 9.0/m before the chicane and ramped down after the chicane to zero at the entrance to the second bending magnet. The initial transverse distribution is a uniform round cross section with 1 mm rms size and 0.7 mm mrad transverse emittance. The initial uncorrelated energy spread is 2 keV.

To verify the suppression of the microbunching instability using the above scheme, we simulated an electron beam with an initial 1% current modulation at 50 μm wavelength transporting through the accelerator system in Fig. 1 with and without including the two bending magnets using a multiparticle tracking code IMPACT [12]. Figures 3 and 4 show the final longitudinal phase space distributions (after removing the chirp) and the projected current profiles at the exit of the accelerator system without and with two bending magnets. It is seen that without using the bending magnets, there is strong modulation in the final

FIG. 2 (color online). Microbunching gain spectrum with (solid line) and without (dashed line) the use of the bending magnets.
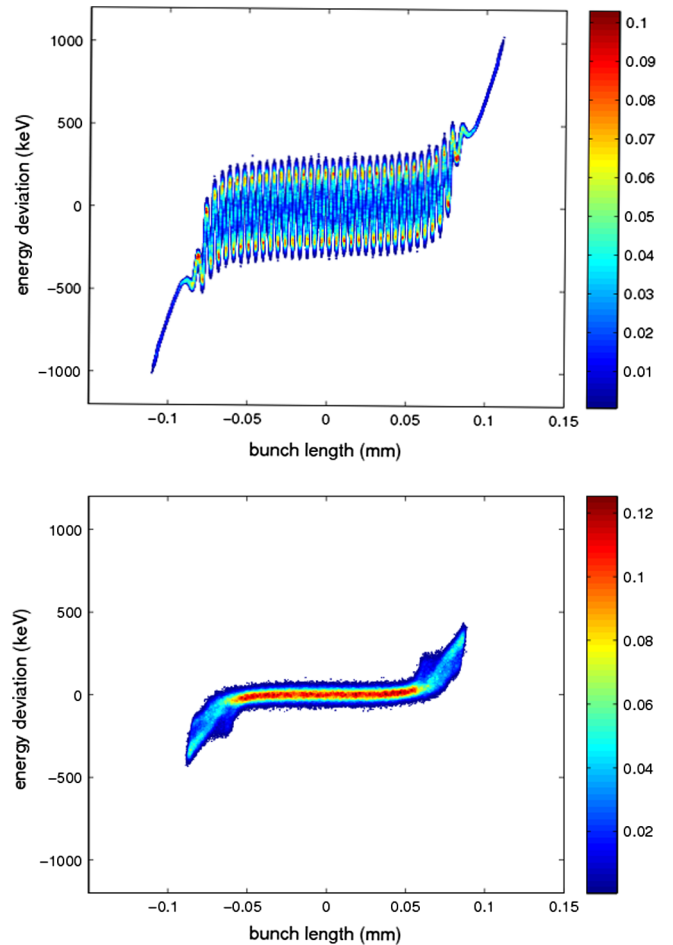

FIG. 3 (color online). Final longitudinal phase space without (top plot) and with (bottom plot) initial and final bending magnets.
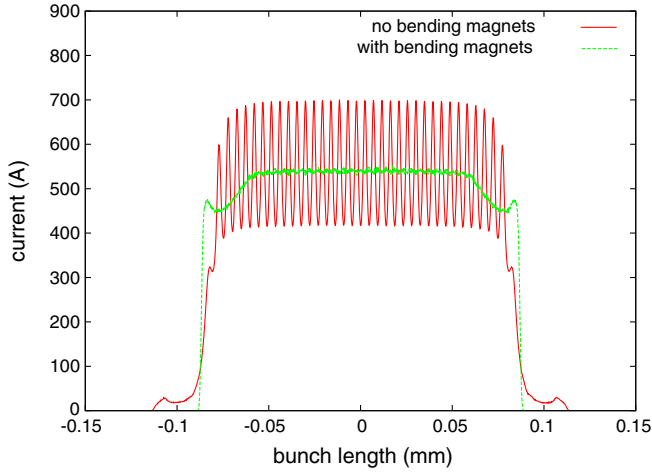
FIG. 4 (color online). Final projected current without (solid line) and with (dashed line) initial and final bending magnets.

phase space distribution. The initial current modulation is amplified by more than a factor of 25 due to the micro-bunching instability driven by the space-charge effects. With the two bending magnets, the microbunching insta-bility is significantly suppressed and the final modulation is barely noticeable.

The use of bending magnets not only suppresses the microbunching instability inside the accelerator system but also significantly reduces the final uncorrelated energy spread in comparison with the laser heater scheme. Figure 5 shows a comparison of the final energy spread without using the bending magnets but with an initial 8 keV uncorrelated energy spread from a laser heater and with the bending magnets but with an initial 2 keV uncor-related energy spread. It is seen that the final uncorrelated energy
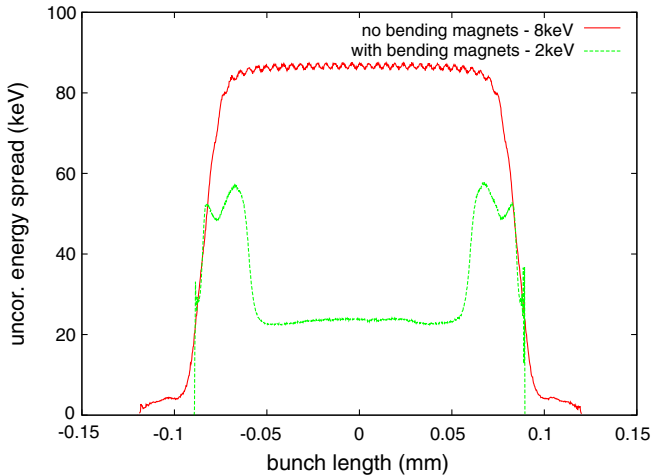

FIG. 5 (color online). Final uncorrelated energy spread with-out using bending magnets but with an initial 6 keV uncorrelated energy spread from the laser heater (solid line), and with bending magnets but with an initial 2 keV uncorrelated energy spread (dashed line).

energy spread using two bending magnets is only about 20 keV while the final energy spread with the laser heater reaches more than 80 keV. This low final uncorrelated energy spread (i.e., the initial uncorrelated energy spread times the compression factor) of the electron beam will help seeded FEL applications to generate high harmonic, short-wavelength x-ray radiation.

The use of bending magnets helps suppress the micro-bunching instability inside the accelerator transport sys-tem. However, it also results in finite dispersion inside the transport system. This will cause horizontal displacement of the longitudinal beam slices. Such off-axis displacement of individual slices can couple with the accelerator trans-verse structure wakefield to cause beam breakup and emit-tance growth. In the following, we will evaluate this effect using an analytical model. The equation of motion govern-ing the center displacement $x(s, z)$ of a slice along the beam can be written as [14]

$$\frac{d}{ds}\left(\gamma(s)\frac{d}{ds}x(s, z)\right) + K_0^2\gamma(s)x(s, z) = F_x(s, z), \quad (11)$$

where z is the longitudinal position with respect to the head of the beam, K_0 is the constant transverse focusing wave number resulting from a smooth approximation to the external focusing lattice, and F_x is the force caused by the transverse wakefield, which is given by

$$F_x(s, z) = \frac{q}{mc^2}\int_0^z \rho(z')W_\perp(z - z')x(s, z')dz', \quad (12)$$

where ρ is the electron beam charge line density and $W_\perp$ is the transverse structure wakefield. We assume that the energy of the beam increases linearly with distance and the focusing strength increases with the same scale as the energy, so that K_0 is kept constant. Using a first-order perturbation method to solve Eq. (11), we obtain the evo-lution of each slice center as

$$x(s, z) = x_{ds}(s, z) + \Delta x(s, z). \quad (13)$$

Here x_{ds} denotes the slice center evolution without the effect of the transverse wakefield and is given by

$$x_{ds}(s, z) = \sqrt{\frac{\gamma_0}{\gamma(s)}}\left[x_{ds}(0, z)\cos(K_0 s) + x'_{ds}(0, z)\frac{\sin(K_0 s)}{K_0}\right], \quad (14)$$

where γ_0 is the relativistic factor at the entrance of the focusing section, $\gamma(s)$ is the relativistic factor at a distance s into the focusing section, and $x_{ds}(0, z)$ and $x'_{ds}(0, z)$ denote the initial slice center displacement and divergence due to the finite energy spread and emittance of the beam caused by the dispersion of the first bending magnet. Finally, Δx denotes the slice center deviation contributed by the transverse wakefield effect and is given by

$$\Delta x(s, z) = \int_0^s ds' \frac{\sin[K_0(s - s')]}{K_0\sqrt{\gamma(s')\gamma(s)}} W(s', z), \quad (15)$$

where

$$W(s', z) = \frac{q}{mc^2} \int_0^z \rho(z')W_\perp(z - z')x_{ds}(s', z')dz'. \quad (16)$$

The slice center deviation will grow with the length of the transport system. The final electron beam projected relative emittance growth due to the slice center offset is about $(\sigma_{\Delta x}^2 \sigma_{x'}^2 + \sigma_{\Delta x'}^2 \sigma_x^2)/(2\epsilon_x^2)$, where $\sigma_{\Delta x, x'}$ are the rms spread of the slice center location and divergence, $\sigma_{x, x'}$ are the rms spread of the beam horizontal location and divergence without the slice center offset, and ϵ_x is the final unnormalized horizontal emittance without the slice center offset. Using the transverse wake function $W_\perp$ for a Tesla cavity and the parameters in the preceding example, the estimated relative emittance growth at the end of the system caused by the transverse wakefield will be about 5×10^{-4}. Here, we have neglected the contribution of the transverse wakefield effects inside the first short section and used the initial slice center displacement and divergence at the beginning of the second section, which has a very small amplitude in the core region and increases to a maximum of a few millimeters near the edge of the distribution. The analytical estimate of the transverse wakefield effect was verified using a direct numerical simulation.

The presence of an accelerating structure before and after a single bending magnet in the above scheme might cause extra emittance growth due to the energy jitter. By using a small bending angle for the second bending magnet, one can significantly reduce the effect of the energy jitter induced by the cavities between the two magnets. For the above numerical example, with a relative energy jitter of 10^{-4}, the final relative divergence fluctuation is on the order of 10^{-3}. In addition, the energy jitter of the beam before the first bending magnet results in centroid offset fluctuation. This might result in horizontal emittance growth due to the presence of the transverse wakefield.

Assuming 10^{-4} relative energy jitter before the first bending magnet, this will only lead to 10^{-5} relative emittance growth which is much smaller than that from the beam itself.

[1] M. Borland *et al.*, Nucl. Instrum. Methods Phys. Res., Sect. A **483**, 268 (2002).

[2] E. L. Saldin, E. A. Schneidmiller, and M. V. Yurkov, Nucl. Instrum. Methods Phys. Res., Sect. A **528**, 355 (2004).

[3] Z. Huang, M. Borland, P. Emma, J. Wu, C. Limborg, G. Stupakov, and J. Welch, Phys. Rev. ST Accel. Beams **7**, 074401 (2004).

[4] M. Venturini, Phys. Rev. ST Accel. Beams **10**, 104401 (2007).

[5] R. A. Bosch, K. J. Kleman, and J. Wu, Phys. Rev. ST Accel. Beams **11**, 090702 (2008).

[6] Z. Huang *et al.*, Phys. Rev. ST Accel. Beams **13**, 020703 (2010).

[7] L. H. Yu, Phys. Rev. A **44**, 5178 (1991).

[8] C. Behrns, Z. Huang, and D. Xiang, Phys. Rev. ST Accel. Beams **15**, 022802 (2012).

[9] Z. Huang and K-J. Kim, Phys. Rev. ST Accel. Beams **5**, 074401 (2002).

[10] S. Heifets, G. Stupakov, and S. Krinsky, Phys. Rev. ST Accel. Beams **5**, 064401 (2002).

[11] S. Di Mitri, M. Cornacchia, S. Spampinati, and S. Milton, Phys. Rev. ST Accel. Beams **13**, 010702 (2010).

[12] J. Qiang, R. Ryne, S. Habib, and V. Decyk, J. Comput. Phys. **163**, 434 (2000).

[13] J. Qiang, R. D. Ryne, M. Venturini, A. A. Zholents, and I. V. Pogorelov, Phys. Rev. ST Accel. Beams **12**, 100702 (2009).

[14] A. W. Chao, B. Richter, and C-Y. Yao, Nucl. Instrum. Methods **178**, 1 (1980).